Development of Experimental Apparatus for Modification and Characterization of Mechanical Behaviour of Aluminum Alloys

Pedro Filipe Gonçalves de Barros
pedrofbarros@tecnico.ulisboa.pt

Instituto Superior Técnico, Universidade de Lisboa, Portugal

December 2021

Abstract

In this work, a test bench was developed for the characterization of materials processed by a severe plastic deformation (SPD) process, Equal Channel Angular Pressing (ECAP). For this purpose, a uniaxial compression tool already existing at the Machining and Micro-Manufacturing Laboratory (LabM3) was improved and instrumented. This tool was coupled to a crankshaft type press. It was also developed an ECAP tool, which was coupled to a manual action hydraulic press. The two machines were installed on the bench. Mechanical tests on aluminum alloy AA 1050 were carried out in order to validate the uniaxial compression tool. Then, it was performed an analysis of the effect of SPD on pure aluminum (Al 99.999%). Some of the specimens were annealed at low temperature. Finally, the hardness and response of the specimens to compression were analyzed, seeking to understand the effects of ECAP and annealing on this material.
Keywords: Plastic deformation, ECAP, uniaxial compression, hardness, mechanical behavior, aluminum.

1. Introduction

Aluminium is widely used in many applications, however this material does not meet the required mechanical resistance. Over the last decades, it has been considered that fine crystal grains produced by severe plastic deformation (SPD) lead to an extraordinarily high metal strength. Looking to that, the main objective of this work is to create an apparatus that allows to deform plastically materials throw an SPD process denominated ECAP, and then make the mechanical characterization of these materials. The studied materials during this investigation were pure aluminium (Al 99,999%) and aluminium alloy AA 1050.

Regarding the aim of this work, an ECAP tool was manufactured in order to make the SPD process possible. Another machine that already existed in LabM3, the uniaxial compression tool, was improved and instrumented with a load cell and a displacement sensor in order to allow the carrying out of experimental tests and take the appropriate measurements. After that, it was necessary to validate the machine. It was done using samples of aluminum alloy AA 1050, which behaviour is well known. Those samples were tested using the uniaxial compression tool and then the results were compared to those obtained by Reis [6].

Once the uniaxial compression tool was functional, the materials pretended to be analyzed were prepared. The samples of pure aluminium (Al 99,999%) and aluminium alloy AA 1050 were manufactured and then processed by ECAP. After the ECAP process, specimens were made. Some of the specimens of pure aluminium (Al 99,999%) were annealed at low temperature, 175 ℃ during 30 minutes as Koizumi et al. [5] did in their research. The compression tests were carried out in uniaxial compression tool and the Vickers hardness tests were also carried out using a harness meter.

This work is organised in six sections, starting by the present introduction, being followed by the background, implementations, methods and materials, results and conclusions.

2. Background

This section starts with a brief presentation of the mechanical tests used to evaluate the mechanical behaviour of the material. Afterwards, it is made a description of the theoretical concepts of ECAP and all the parameters that have influence in the process. Then, influence of heat treatment in the material´s microstructure and in the stress relief is reviewed. Finally, it is made an analysis on some relevant studies regarding this subject.

2.1. Mechanical Tests

The uniaxial compression test consists on smashing a specimen between two flat plates. In this type of tests, one of the plates is usually stationary, whereas the other is moved while the gap between them is shortened, as seen in Figure 1. The the cross section diameter of the specimen increases while a height reduction occurs.

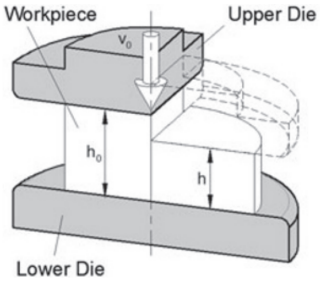

Figure 1: Schematic representation of a uniaxial compression test [8].

The dimensions of the specimen are an important contributing factor to friction. When aspect ratio < 1, the minimum increase in friction leads to a significant rise in pressure. On the other hand, if aspect ratio > 3, some fails such as bending or buckling can occur in specimen [2].

The stress-strain curves obtained by compression tests reveal some information concerning the mechanical properties of the material. The stress and strain are given by equations (1) and (2), respectively.

$$\sigma = \frac{F}{A_i} \tag{1}$$

$$\varepsilon = -\int_{h_0}^{h_i} \frac{1}{h}\, dh = \ln\left(\frac{h_0}{h_i}\right) \tag{2}$$

Hardness is another important property of the materials. It can be defined as the resistance of the material to permanent deformation. The hardness test considered in this investigation was the Vickers hardness test. Its value is given by equation (3). It depends on the mean diagonal of the indentation d_m $[mm]$ and the force applied P $[N]$.

$$HV = 1.854\frac{P}{d_m^2} \tag{3}$$

2.2. Fundamentals of ECAP

The ECAP die has an internal channel, which cross section can be either rectangular or circular. A schematic representation of the process and nomenclature is presented in Figure 2. The channel has a curvature of angle ϕ, which values typically range between 90° and 150° and defines how severe the shear deformation is, as it is the main parameter to influence the total strain imposed in each pass. The channel may also have an outer corner angle ψ.

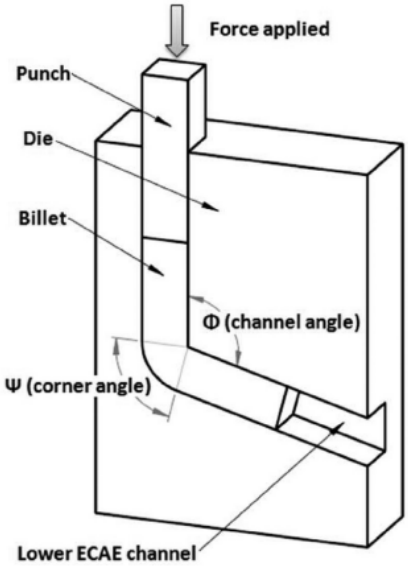

Figure 2: Schematic representation of ECAP process [1].

The effect of the angles on the equivalent effective strain is expressed by equation (4), which is an accumulative strain of the operation. The factor N is the total number of passes [4]. Among all the possibilities, in a wide number of investigations an angle $\phi = 90°$ is preferred, in spite of the fact that it requires less force when using larger angles. The corner angle ψ has less influence on the strain, however it has been found that smaller corner angles maximize the homogeneous portion of the billet. Xu and Langdon [11] consider that $\psi = 20°$ is the best option when projecting the ECAP tool and it is also said that the tool should be made in a single piece in order to avoid extrusion of the material between the modules.

$$\varepsilon_N = \frac{N}{\sqrt{3}}\left[2\cot\left(\frac{\phi+\psi}{2}\right) + \psi\csc\left(\frac{\phi+\psi}{2}\right)\right] \tag{4}$$

The billet is expected to leave the die with a grain refinement that can be at the submicrometer or nanometer level [11], depending on the number of passes and other parameters.

According to Agwa et al. [1], a friction coefficient of $\mu = 0,3$ is ideal. Friction has a determinant role on homogenising the billet, however, higher friction leads to more loading and also some risk of damaging the tool.

Another important factor which greatly influences the mechanical properties of the samples after

the ECAP process is the orientation changing between passes. It can be done according to four different routes. Each one promotes different textures and microstructures. In route A, the position of the sample is kept the same between passes. When using Route B_A, the sample is rotated 90° around its longitudinal axis. Between each pass the rotation's direction is alternated. For route B_C, the sample is rotated 90° around its the longitudinal axis between passes, always in the same direction. In route C the sample is rotated 180° around the longitudinal axis between passes. A schematic representation of the four routes is presented in Figure 3. Venkatachalam et al. [10] found out that the route that improves the most the mechanical resistance of the aluminium alloy 2014 is the route B_C.

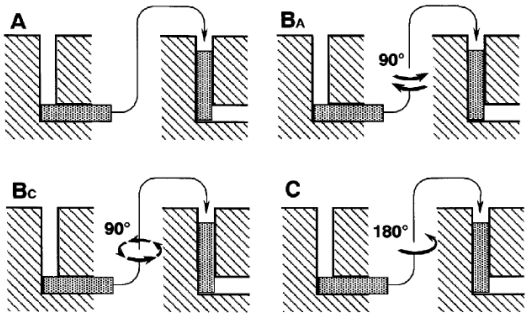

Figure 3: Schematic representation of the four possible ECAP routes [9]

ECAP is an operation based on the combination of two types of strengthening mechanisms: grain size reduction and strain hardening. The initial microstructure is a factor which greatly influences these mechanisms. The case in study, aluminium, is a polycrystalline metal with a FCC crystal structure.

The mean grain size in polycrystalline metals influences the mechanical properties. Grains with different crystallographic orientations are separated by a grain boundary, which works as an obstacle to dislocation motion. The dislocation when passing to the next grain must change its direction, so that it becomes more difficult when the misorientation angle between grains is more pronounced. Grain boundaries also create slip plane discontinuity. It is important to refer that pile-up dislocations can occur at the boundary, not passing to the next grain. All these aspects are obstacles to deformation, so fine-grained structures are mechanically more resistant and harder than coarse grain structures.

The mechanical behaviour is also influenced by the dislocation motion. The capability of dislocations to pass from grain to grain influences the ease of a metal to deform plastically. If this mobility is reduced, greater forces will be needed to permanently deform the material. This increase in force results in higher yield and tensile strength. In this case, it has occurred strengthening due to strain hardening.

Cold working promotes the formation of new dislocations, increasing its density per unit of volume. As a result the distance between dislocations is shortened. Normally, when dislocations are forced to interact with each other, the forces tend to be repulsive. So, the dislocation density leads to hardening due to resistance to dislocation motion. However, the ductility decreases [3].

2.3. Annealing at Low Temperature

Koizumi et al. [5] in their investigation submitted pure aluminium (Al 99,7%) to an ECAP tool of channel angel $\phi = 90°$ and corner angle $\psi = 36,87°$. The process was realized according to route B_C at room temperature. The strain rate of the process was $0,3$ to $0,5$ s^{-1} approximately. The samples were processed with different numbers of ECAP passes: 0 passes, 1 pass, 4 passes and 8 passes. Some of the samples processed with 8 ECAP passes were subsequently annealed at 175 ℃ for $0,5$ h or 6 h (henceforth referred to as "8 passes-O1" and "8 passes-O2", respectively). Then, the billets were submitted to tensile tests. In the tensile testes, two strain rates ($\dot{\varepsilon}$) were considered: one is an extraordinarily low strain rate of 4×10^{-7} s^{-1}, and the other is a strain rate of 1×10^{-2} s^{-1}, which lies within a range generally used for normal tensile tests.

In the low-strain-rate tests ($\dot{\varepsilon} = 4 \times 10^{-7}$ s^{-1}), which is represented in the graph of Figure 4, the tensile flow stress of the sample "0 passes" was quadrupled by the first ECAP processing. In the subsequent ECAP processes, the flow stress was markedly decreased. Significant softening by SPD was observed for 1 to 8 ECAP passes. Grain size strengthening was not observed in the as ECAP processed samples. The subsequent low-temperature annealing approximately doubled the flow stress of the sample "8 passes".

For the normal strain rate test ($\dot{\varepsilon} = 1 \times 10^{-2}$ s^{-1}) it was observed that repeated ECAP processes gradually augment the strength of the sample, but the subsequent annealing slightly decreases it. So in this study, it was concluded that grain refining promoted by SPD itself strengthens the material. However, it is obvious that this understanding is erroneous as the results presented in the graph of Figure 4 show softening by SPD [5].

3. Implementation

This section focus on the development of the experimental apparatus. In order to have a support for the necessary machines it was necessary to install an experimental test bench. Afterwards in this section, the machines used in this work will be described as

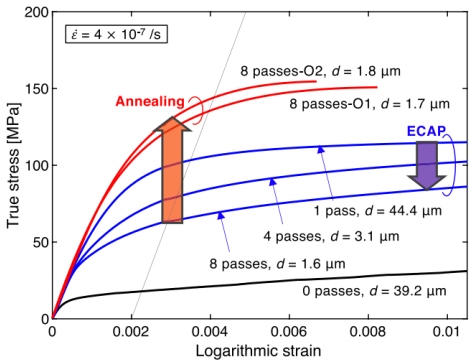

Figure 4: Experimental curve of true stress versus logarithmic strain in uniaxial tension at strain rate of $\dot{\varepsilon} = 4 \times 10^{-7}\ s^{-1}$. [9]

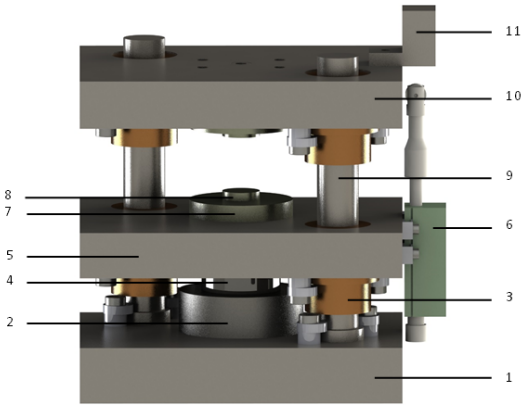

Figure 5: Uniaxial compression tool CAD: 1 - Tool base; 2 - Load cell base; 3 - Bushing; 4 - Load cell; 5 - Bottom platen; 6 - Displacement sensor; 7 - Steel platen; 8 - Compression platen; 9 - Guide; 10 - Top platen; 11 - Actuator.

well as the manufactured tools.

3.1. Crankshaft Press

In order to perform the uniaxial compression tests, a press whose operating mechanism is crankshaft type was selected. This press is able to perform tests with a range of strain rates from $\dot{\varepsilon} = 2 \times 10^{-1}\ s^{-1}$ to $\dot{\varepsilon} = 3\ s^{-1}$. In this work the minimum strain rate was used. This press achieves a maximum load of 40 kN. Some improvements were made in order to minimize existing slacks.

3.2. Uniaxial Compression Tool

The tool to carry out the uniaxial tests is represented in Figure 5, which was developed by Santos [7]. The components are also represented and described. This tool was developed in order to ensure the parallelism of the platens and the correct data measurements of the tests: force and displacement. It is important to note that the compression plates were made in hard metal (tungsten carbide), since it can support all the effort involved in the compression. In addition, some improvements were made, such as the position of the sensors, in order to have a more clear and reliable data acquisition.

3.3. Instrumentation and Data Acquisition

In order to measure the displacement and the force during the tests, a displacement sensor and a load cell were installed, respectively. The outputs of these sensors are analog signals in voltage [V]. This means that sensors should be connected to a data acquisition system (DAQ), which is connected to a computer. A *National Instruments NI-USB 6001* DAQ was used. It allows the computer to read the data from the sensors. In addition a LabVIEW program was developed in order to read ad register the output of the DAQ.

In order to supply the required power to the sensors, it was built a box with all the components, such as two power supplies, for both displacement and load sensors, and a weight transmitter necessary for the load cell. In addition, this box allows the sensors to be connected and disconnected through connectors instead of soldering the cables. This represents a portable solution, being possible to take the box away, for example when performing calibration. A LabVIEW program was developed to read and save the data from the sensors. In Figure 6 is presented a scheme of the data acquisition system .

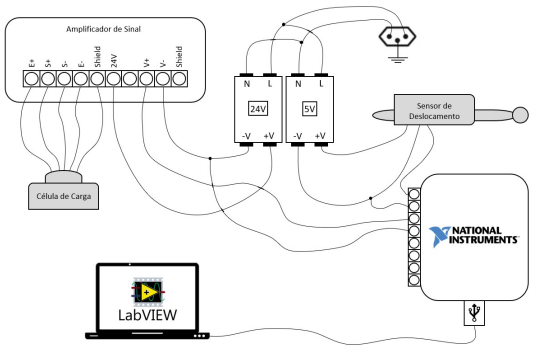

Figure 6: Data acquisition system representation.

To perform the load cell calibration, a system was developed. This system is based on the lever principle. The applied force in both sides of the lever is given by the product of the magnitude of the force and its effort arm (the distance of its point of application from the fulcrum). So, for equilibrium, the force in the bigger arm is lower than the force in the smaller arm. In Figure 7 is presented a scheme of the developed system. This system has a factor of multiplication of $f = 24,96$. The calculation is present in equation (5).

$$f = \frac{1248}{50} = 24,96 \tag{5}$$

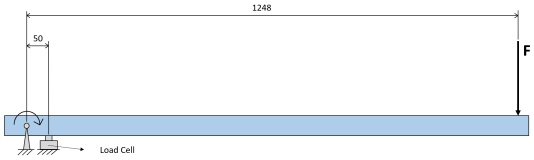

Figure 7: Cell load calibration system representation.

3.4. ECAP Tool

Before the development of a new ECAP tool, it was tested the one already existing in LamM3. However, when tested the tool revealed some fails. This tool was manufactured by modules. When tested, the material flowed through the surfaces between the modules of the die, Figure 8. In addition, reverse extrusion has occurred between the channel surface and the punch. Due to this, there were several problems, such as damages in the die and in the punch.

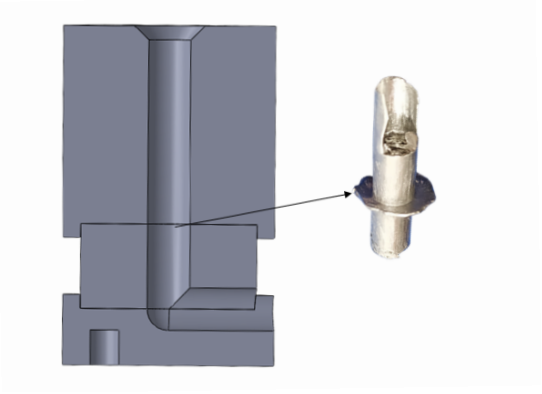

Figure 8: Material flow between modules.

In order to solve the problems, a new ECAP tool was designed and manufactured. Following the Xu and Langdon [11], the new ECAP tool is a solid die. The channel angle is $\phi = 90°$ and the outer corner angle is $\psi = 36,87°$. The tool was made at NOF (*Núcleo de Oficinas*) at IST. Then, the die was mounted on structure that ensures straight movement, similar to the one presented above in section 3.2. The scheme of the tool is presented in Figure 9.

In order to carry out the process, this tool was mounted in a manual action hydraulic press. The press used is *MEGA PRS15*, which achieves a maximum load of 15ton.

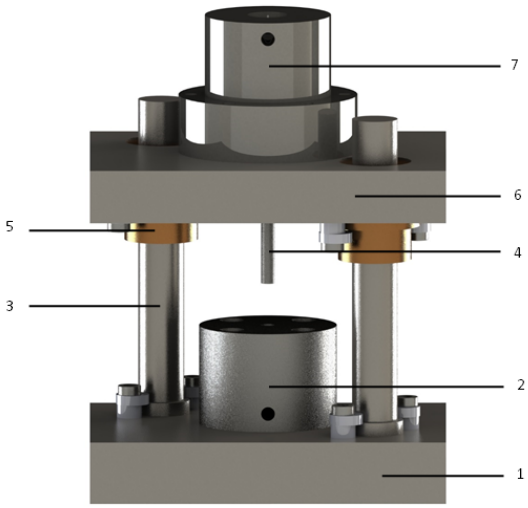

Figure 9: ECAP tool CAD: 1 - Tool base; 2 - ECAP die; 3 - Guide; 4 - Punch; 5 - Bushing; 6 - Top platen; 7 - Connection to the press.

4. Materials and Methods

In this section the materials and the methods used to carry out this investigation are explained. One of the objectives of this work is to analyze the influence of the ECAP process on mechanical resistance of pure aluminium (Al 99,999%). Before any test, the uniaxial compression machine had to be validated. Regarding to this, also billets of aluminium alloy AA 1050 were used, since its behaviour is well known on the literature and it had already been tested with different equipment in the IST, allowing to make comparisons between results.

All of the specimens used in uniaxial compression tests have a cylindrical shape. All of them were manufactured taking into account the aspect ratio. Aspect ratio should be equal or greater than one and less than three, in order to avoid friction or buckling and bending problems [2]. The specimens were made with an aspect ratio near to one.

First of all, the specimens of aluminum alloy AA 1050 were made with a diameter of 6 mm, in order to validate the uniaxial compression tool. It was also manufactured a billet of this material with 6 mm diameter and 35 mm length, with the purpose of being processed by ECAP. Both specimens and billet were manufactured using the micro-machining test center *PROTEO* existing in LabM3. Then, the hardness of aluminum alloy AA 1050 were measured using a hardness meter *HARDRULER HVS-1000* existing in LabM3.

Afterwards, the billets of pure aluminium (Al 99,999%) with 35 mm length were manufactured from a bar with 6 mm diameter, using the micro-

machining test center *PROTEO*. Then, it was ECAP processed into different conditions: 1, 2, 4 and 8 passes. The pure aluminium (Al 99,999%) billets after ECAP can be seen in Figure 10. The billet of aluminium allooy AA 1050 was also ECAP processed at condition 6 passes.

Figure 10: Pure aluminium (Al 99,999%) billets after ECAP: (left to right) 1 pass; 2 passes; 4 passes; 8 passes

The ECAP process occurred at room temperature at a strain rate of approximately $0,3$ to $0,5\ s^{-1}$. In order to prevent damages on punch and die due to friction, graphite was used as lubricant. In spite of being stated at section 2 that route B_C is the best option, in the present investigation the route selected is route A. The selection was made in order to make the process easier.

After ECAP process, the billets were cut into specimens using a EDM machine *Charmilles Robofil 190* at NOF. The surfaces of specimens were polished, in order to be clean and without irregularities not to compromise the following tests. Some of the specimens were annealed at low temperature 175 ℃ for 30 minutes, as Koizumi et al. [5].

Then, the hardness of all specimens were measured using a hardness meter *HARDRULER HVS-1000*.

Finally, after having validated the uniaxial compression machine, all of the specimens of pure aluminium (Al 99,999%) and aluminium alloy after ECAP and annealing were compressed using a strain rate $\dot{\varepsilon} = 2 \times 10^{-1}\ s^{-1}$. After compression, hardness tests were performed at all compressed specimens. The results will be discussed in section 5.

5. Results

This section presents the results of the performed tests. In the first part is presented the validation of the machine and in the second part the data acquired from compression and hardness tests for pure aluminium (Al 99,999%) and aluminium alloy AA 1050.

5.1. Machine Validation

After all the improvements made to the machine, tool and data acquisition system, it was necessary to validate it.

The calibration was made using calibrated height specimens. The data was acquired and treated in order to obtain a curve with the values. In Figure 11 is presented a graph with the curve obtained as well as the previous one, obtained before any improvement.

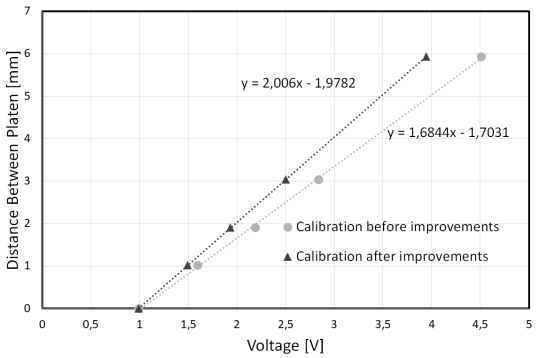

Figure 11: Calibration curves of displacement senor after and before improvements.

As it can be seen, the values after improvements are as expected. The displacement sensor has a range of 0 to 10 mm and an output voltage of 0 to $5V$. It is linear. So, it is expected that the curve is linear of slope equal to 2.

Then, as done previously for the displacement sensor, the load cell was also calibrated. To perform it, the system developed on subsection 3.3 was used. The calibration was done until $24kN$, since the range of force values during compression tests are lower than this. The curve obtained as well as the slope are shown on graph of Figure 12.

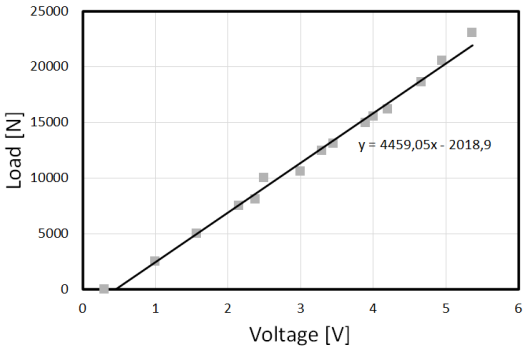

Figure 12: Calibration curve of load cell senor after improvements.

It is known that the values acquired by the data acquisition system are affected by the elasticity of the machine. In order to know the values of the deformation to possibly compensate the results for uniaxial compression tests, a uniaxial compression test was performed without any material under the

platen, just platen against platen. From this test the values of force and displacement were acquired and then it was possible to make a curve. This curve is presented on graph of Figure 13. The deformation values acquired were reduced in 65% (according to previou values) due to the improvements.

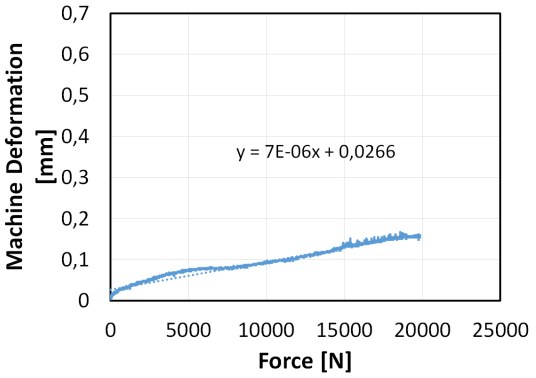

Figure 13: Elastic deformation curve of the machine.

After all the validation, a uniaxial compression test of an aluminium alloy AA 1050 specimen was carried out. The curve obtained was compared to the one obtained previously by Reis [6] in order to validate the machine. As seen in graph of Figure 14, the curves are very close, having a maximum error below 5%.

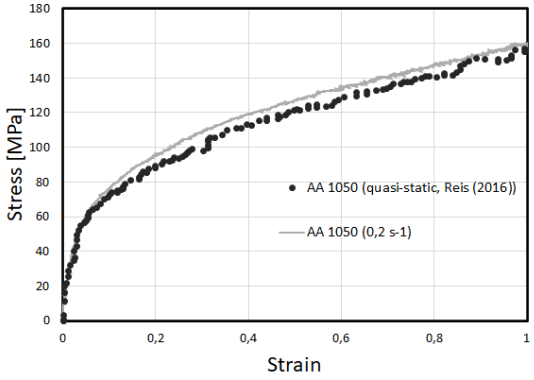

Figure 14: Strain-stress curves of aluminium alloy AA 1050 obtained in this work and by Reis [6].

5.2. Evolution of Stress with Strain Variation

The true stress versus true strain curves for pure aluminium (Al 99,999%) are presented in the graph of Figure 15. The curves of the graph refer to the material in the conditions: 0 passes, 1 pass, 2 passes, 4 passes and 8 passes after plastic deformation at strain rate $\dot{\varepsilon} = 2 \times 10^{-1}\ s^{-1}$.

The results show a substantial increase in stress flow after first pass. In the following conditions (2, 4 and 8 passes) the yield and flow stress decrease, which suggests material softening.

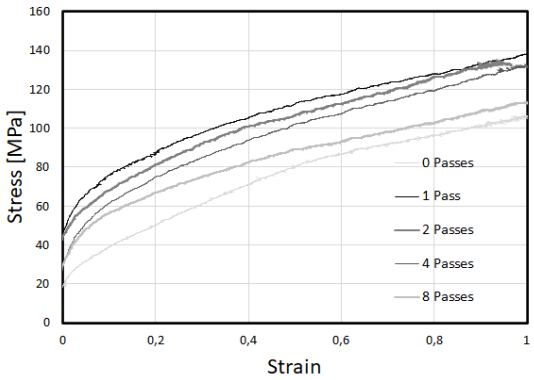

Figure 15: Strain-stress curves of pure aluminium (Al 99,999%) after ECAP, plastic component.

The specimens submitted to annealing at low temperature were compressed too at strain rate $\dot{\varepsilon} = 2 \times 10^{-1}\ s^{-1}$. Figure 16 shows the graph with the curves obtained for the uniaxial compression of the specimens annealed at the following conditions: 1, 2, 4 and 8 passes.

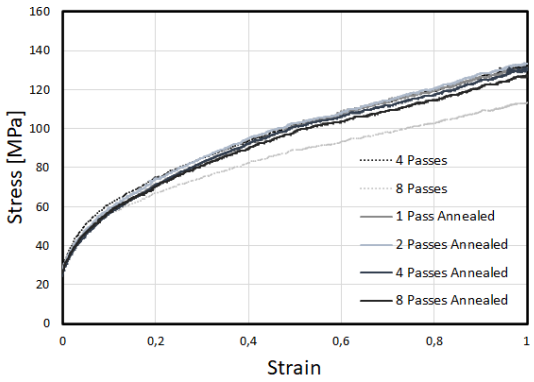

Figure 16: Strain-stress curves of pure aluminium (Al 99,999%) after ECAP annealed, plastic component.

Looking to the graph it is possible to see that there was a stress flow increase of the specimen in condition 8 passes after annealing. The specimens in other conditions (1, 2 and 4 passes) reveal softening, since stress flow decreases. It is also visible the convergence of values in all conditions for values very close.

The aluminium alloy ECAP processed specimens were obtained only at 6 passes condition. The curves obtained for compression at strain rate $\dot{\varepsilon} = 2 \times 10^{-1}\ s^{-1}$ are present in graph of Figure 17.

Looking to the graph, is possible to see a yield stress increase of about 3 times the value for the initial condition of the material. It is also visible

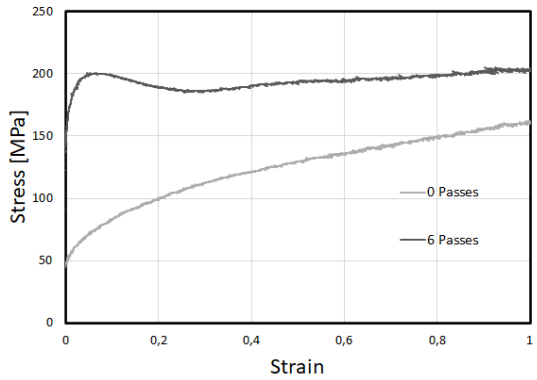

Figure 17: Strain-stress curves of aluminium alloy AA 1050 after ECAP, plastic component.

that after strain $\varepsilon = 0,2$, the flow stress of the 6 passes condition material remains almost constant. On the other hand, this value increases with strain.

5.3. Evolution of harness with ECAP Passes

Before and after each uniaxial compression test, hardness were measured for all conditions on previous subsection. The graph on Figure 18 shows the evolution of hardness for pure aluminium (Al 99,999%) with the number of ECAP passes, N. The curves presented in this graph refer to this material before and after the uniaxial compression test in each condition.

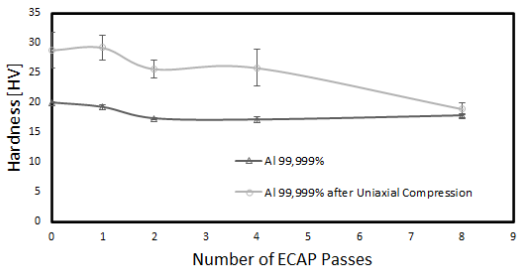

Figure 18: Hardness evolution with number of ECAP passes (before and after uniaxial compression) for pure aluminium (Al 99,999%).

The material after ECAP process presents softening after the first pass, followed by a smooth hardness increase. It is important to know that the initial value of hardness (≈ 20 HV) is slightly above the theoretical value at its annealed condition (15 HV). The material was used as provided by the supplier, according to which the material was annealed at 400 ℃ during 1 h. It would be expected to obtain values of hardness from 15 to 16 HV for the condition 0 passes. It can be due to the aging of material for the time it was stored before the use. After uniaxial compression, the hardness values for all conditions increase, except for the 8 passes condition, whose values converge for very close values before and after uniaxial compression, $17,8$ HV and $18,95$ HV, respectively.

The hardness values for pure aluminium (Al 99,999%) annealed are presented in graph of Figure 19. After annealing, the hardness values remains almost constant throughout the number of ECAP passes. The values ranges from $16,3$ HV to $17,88$ HV. After compression, the material presents a decrease between the first and the second pass, followed by an increase for condition 4 passes. Then there is a smooth decrease in hardness for 8 passes condition.

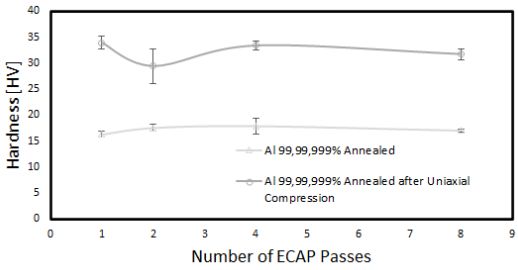

Figure 19: Hardness evolution with number of ECAP passes (before and after uniaxial compression) for pure aluminium (Al 99,999%) annealed.

Figure 20 presents the hardness graph for the aluminium alloy AA 1050 according to the number of ECAP passes, before and after uniaxial compression. This material was only ECAP processed at 6 passes condition. Regarding the graph, it is notorious an increase in hardness with ECAP. The increase is more expressive before uniaxial compression. The hardness values for 6 passes condition converge to close values, $51,38$ HV and $53,22$ HV before and after uniaxial compression, respectively.

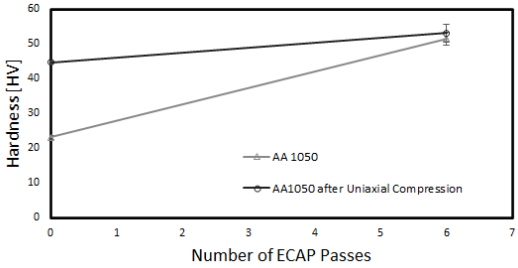

Figure 20: Hardness evolution with number of ECAP passes (before and after uniaxial compression) for aluminium alloy AA 1050.

6. Conclusions

The test bench, as well as the all the equipment were successfully installed and proved to be functional, through validation tests. The ECAP tool

was successfully manufactured and proved robust, making the ECAP process possible.

Both material, pure aluminium (Al 99,999%) and aluminium alloy AA 1050, were ECAP processed and tested through uniaxial compression test at strain rate $\dot{\varepsilon} = 2 \times 10^{-1}\ s^{-1}$. Also hardness was measured. For pure aluminium (Al 99,999%) it was noticed a reduction in mechanical strength after ECAP processing. However, after the first pass (2, 4 and 8 passes) it was observed a flow stress decreasing with the number of ECAP passes. Nonetheless, these values remained always higher than the initial condition. The hardness values decreased along the number of ECAP passes. This supports the decrease on stress flow.

The specimens annealed after ECAP, presented an increase in strength for the 8 passes condition when compared to the value for the specimen in the same condition not annealed. This is in accordance with the results of Koizumi et al. [5]. In the other conditions, this did not happen. There was a softening after annealing. Hardness values did not vary.

The aluminium alloy AA 1050 after 6 passes by ECAP presents a significant increase on yield and flow stress. The same happened for hardness values. There is a convergence on hardness values observed for 6 passes condition before and after uniaxial compression.

A future work could pass by repeat this investigation for pure aluminium (Al 99,999%), taking into account that the material may be aged. It is suggested to anneal the material at 400 ℃ for 1 h before ECAP process.

In order to complement the analysis of mechanical properties of ECAP processed material, a fracture test equipment should be added to the test bench developed throughout this investigation.

References

[1] M. Agwa, M. Ali, and A. Al-Shorbagy. Optimum processing parameters for equal channel angular pressing. *Mechanics of Materials*, 100, 09 2016.

[2] L. Alves, C. Nielsen, and P. Martins. Revisiting the Fundamentals and Capabilities of the Stack Compression Test. *Experimental Mechanics*, 51:1565–1572, 11 2011.

[3] W. Callister and D. Rethwisch. *Materials Science and Engineering: An Introduction*. Wiley Global Education, 9^{th} edition, 2014.

[4] Y. Iwahashi, J. Wang, Z. Horita, M. Nemoto, and T. G. Langdon. Principle of equal-channel angular pressing for the processing of ultra-fine grained materials. *Scripta Materialia*, 35:143–146, 1996.

[5] T. Koizumi, A. Kurumatani, and M. Kuroda. Athermal strength of pure aluminum is significantly decreased by severe plastic deformation and it is markedly augmented by subsequent annealing. *Scientific Reports*, 10, 08 2020.

[6] A. P. d. Reis. Efeito de escala na resistência mecânica de materiais. Master's thesis, Instituto Superior Técnico, 2016.

[7] P. M. G. Santos. Ensaios de Compressão Uniaxial: Desenvolvimento de Máquina e Aplicação a Metais e Ligas Metálicas Engenharia Mecânica. Master's thesis, Instituto Superior Técnico, 2019.

[8] C. M. A. Silva, P. A. R. Rosa, and P. A. F. Martins. Innovative Testing Machines and Methodologies for the Mechanical Characterization of Materials. *Experimental Techniques*, 40:569–581, 2016.

[9] R. Z. Valiev and T. G. Langdon. Principles of equal-channel angular pressing as a processing tool for grain refinement. *Progress in Materials Science*, 51:881–981, 2006.

[10] P. Venkatachalam, S. Ramesh Kumar, B. Ravisankar, V. Thomas Paul, and M. Vijayalakshmi. Effect of processing routes on microstructure and mechanical properties of 2014 Al alloy processed by equal channel angular pressing. *Transactions of Nonferrous Metals Society of China*, 20(10):1822–1828, 2010.

[11] C. Xu and T. Langdon. The development of hardness homogeneity in aluminum and an aluminum alloy processed by ecap. *Journal of Materials Science*, 42:1542–1550, 01 2007.